Article

Highly Photoluminescent Nitrogen-Doped Carbon Dots Prepared by Hydrothermal Decomposition of Piperazine Citrate

Min-Cheol Kim [1], Kwang Sik Yu [2], Jwa-Jin Kim [3], Seung Yun Han [2], Nam Seob Lee [2], Young Gil Jeong [3] and Do Kyung Kim [2],*

[1] Department of Mechanical Engineering, Massachusetts Institute of Technology, Cambridge, MA 02139, USA; mincheol@mit.edu

[2] Department of Anatomy, Konyang University, Daejeon 302-718, Korea; withreno@konyang.ac.kr (K.S.Y.); jjzzy@konyang.ac.kr (S.Y.H.); nslee@konyang.ac.kr (N.S.L.);

[3] Department of Anatomy, School of Medicine, Chungnam National University, Daejeon 301-747, Korea; kjj4827@gmail.com (J.-J.K.); ygjeong@konyang.ac.kr (Y.G.J.)

* Correspondence: dokyung@konyang.ac.kr; Tel.: +82-42-600-6445

Abstract: Highly photoluminescent C-Dots are prepared by hydrothermal reaction of citric acid and piperazine as dual reason in both hydrolysis and surface passivation agent along with the N-doping agent. The resulting C-Dots without external passivation showed PL enhancement by electron transfer from C-Dots-donor to piperazine-acceptor with the maximum emission yields of more than 84%. After mixing the prepared C-Dots with the mixture of EtOH and acetone (1:1 vol %), a novel washing process was performed by centrifugation to remove the precursors and by-products. The resulting C-Dots showed much better stability than dialysis. For evaluating the possible application of the C-Dots as a fluorescent biological probe which possess the wide dosing window and multicolor properties. The C-Dots were localized in perinuclear vacuole-like structures with granular pattern in cytoplasm sparing the nucleus. No signs of any morphological deterioration like nuclear shrinkage were observed.

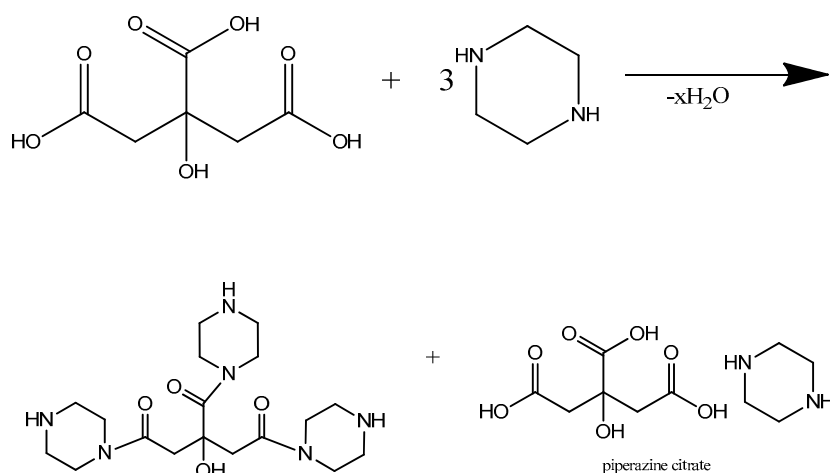**Keywords:** carbon dots; fluorescent; nanoparticles; multicolor imaging; quantum yield

1. Introduction

Recently, photoluminescence (PL) nanoparticles have been intensively studied due to their tunable and unique optical properties such as resistance to photo-bleaching, which has been a common problem for organic PL dyes. Significant effort has been devoted to eliminate the toxicity as well as to find alternative materials while retaining advantageous optical properties of heavy metal based on quantum dots. Among several alternative substances, such as ZnSe, ZnS, InP/ZnS and CuInS/ZnS etc., carbon dots (C-Dots) have been frequently investigated as promising alternative materials due to their superior chemical inertness and biocompatibility with low cytotoxicity. [1]·[2] The fluorescent C-Dots have constitutional compositions of carbon, oxygen and hydrogen with amorphous structure, that is, without discernable crystal lattice. Additionally, the C-Dots exhibited similar conductive characteristics to, crystalline graphite when surrounding conditions, such as the presence of nitrogen, is optimized.[3] The high surface-to-volume ratio of amorphous carbon nanoparticles signifies of their important role in optoelectronic and nanomedicinal applications. The growth of shell molecules on core materials forming heterostructures has been introduced as a successful route in the surface modification of nanoparticles. Core-shell structures are introduced to the field of quantum dots with accounts of improved luminesce quantum yields, decreased fluoresce lifetime, and benefits related to the tailoring of relative band gap positions between the two materials [4].

1   The factors affecting the QY of C-Dots include ion doping, host material, size and shape of
2 nanoparticles, surface defects, external enhancement, etc. Although lots of efforts have been made to
3 enhance the emission efficiency of C-Dots, their QY is still relatively low.[5]
4   Until now, several different synthetic pathway have been developed including pyrolysis of
5 organic molecules[6], laser ablation of carbon target, ultrasound, microwave assisted synthesis etc.
6 To facilitate the PL properties of C-Dots, several strategies have been reported such as oxidation with
7 the acid[7], HNO_3 or with the oxidant, $KMnO_4$, under surface passivation.[8] The C-Dots prepared
8 using different routes are required to process the surface passivation with massive hydroxyl group
9 and the oxidation to enhance the photoluminescence. Sun et al. reported the passivation of surface of
10 C-Dots with PEG_{1500N} resulting in the enhancement of QY from 4 % to about 10 %.[6] A hydrothermal
11 route was used by refluxing a mixed solution containing several lactoses, i.e. α-D-lactose, D-glucose
12 and sucrose, as carbon sources. As the surface passivation reagent, tris(hydroxymethyl)
13 aminomethane (i.e. Tris) were used with a QY of 12.5 %.[9] Liu et al. reported amphiphilic triblock
14 copolymer F127-modified silica spheres as the driving carriers and resols (phenol/formaldehyde
15 resins) as carbon precursors. As a result, QY of the PEG_{1500N}-passivated C-Dots was characterized to
16 be 14.7 %.[1] C-dots were synthesized by hydrothermal reaction of urea and PEG using prolonged
17 time microwave-assisted heating (PT-MAH) method resulting in QY of 17.73%.[10] The QY of 11%
18 was reported by decomposing   citric acid in diethylene glycol bis (3-aminopropyl) ether at 400 °C
19 for 2 hr.[11] An organosilane was utilized as a coordinating solvent to synthesize highly luminescent
20 by pyrolysis of anhydrous citric acid in N-(β-aminoethyl)-γ-aminopropyl methyldimethoxy silane
21 (AEAPMS) at 240 °C for 1 min. The QY of the corresponding C-Dot was reported to be as high as
22 47 %.[12] The same research group reported various silane pre-functionalized CDs (SiCDs), their
23 Ormosil nanohybrid gel glass composites (SiCD-Gel glasses) and macrostructure monoliths (100 %
24 SiCD-Gel glasses). These materials exhibit excellent PL emissions (QY = 47 % for SiCD and 88 % for
25 SiCD-Gel glasses) and broadband optical limiting (OL).[13] Recently, Yang et al. have reported
26 polymer like C-Dots with a QY as high as ca. 80 % by reacting citric acid with ethylenediamine.[14]
27   Here, we propose a simple hydrothermal synthesis of amine terminated C-Dots by employing
28 short chain carboxyl acid as a carbonic core and piperazine as a both hydrolysis and surface
29 passivation agent along with the N-doping agent. The resulting C-Dots without external passivation
30 showed PL enhancement by electron transfer from C-Dots-donor to piperazine-acceptor with the
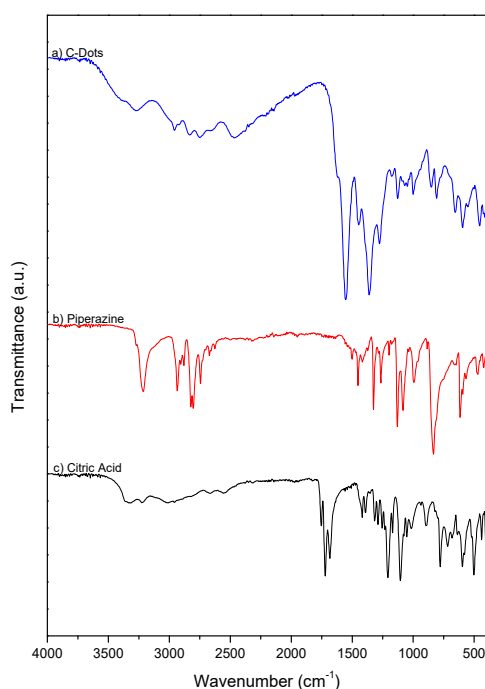31 maximum emission yields of more than 84 %.

32
33   **Scheme 1.** Schematic representation of the chemical reaction between piperazine and citric acid at
34   high temperature and pressure.

35 **2. Results and Discussion**

36 *2.1. Synthesis and characterization of N-doped C-Dots*

37   In general, lanthanide complexes with β-diketone is expected drastically to enhance the
38 luminescence properties. The chelated Eu^{3+} and Tb^{3+} with β-diketone emit characteristic fluorescence

1   for long lifetimes due to intermolecular energy transfer from the excited β-diketone to Eu^{3+} and Tb^{3+}.
2   Additionally, strong chelating ligands such as 2,2′-bipyidine are essential to prepare the fluorescent
3   lanthanide complexes; especially, it is a bidentate chelating ligand, forming complexes with various
4   transition metals. The electronic transitions are attributed to metal-to-ligand charge transfer (MLCT).

5

Figure 1. FTIR spectra of (a) C-Dots prepared at 200 for 5 hrs with a molar ration of citric acid:
piperazine = 1:3, (b) piperazine and (c) citric acid.

8   The luminescence emerges from the electron resonance in benzene molecules. Inspiring from
9   the bipyridine used in lanthanide based luminescence, piperazine was selected as a reducing, N-
10   doping and proton induced electron transfer (PET) agent due to its six-membered ring containing
11   two nitrogen atoms at opposite sites in the ring. The C-dots were synthesized by hydrothermal
12   decomposition of carboxyl group in a small molecule by reacting with amine group in piperazine.
13   The chemical reaction firstly involves condensation of citric acid and piperazine with a release of H_2O
14   at both high temperature and pressure. The overall synthetic procedure is illustrated in Scheme 1.
15   The carboxyl group of the three molecules in citric acid produced three molecules of water and
16   formed peptide bonds by reacting with the amine group in piperazine.
17   FTIR spectra (Figure 1) were analyzed to identify chemical structures after synthesizing the C-
18   Dots. Several drops of the already prepared sample were directly dried on the diamond ATR to
19   examine the chemical species after the hydrothermal reaction. The C-H stretching vibrations of
20   aromatic and hetero-aromatic structure occur in the region of 2,800 - 3,100 cm^{-1}. FTIR spectrum of
21   piperazine shows peaks at 2,936, 2,908, 2,882, 2,826 and 2,802 cm^{-1} , and can be assigned to C-H
22   stretching vibrations. In secondary amine, the symmetrical CH_2 stretching group next to the nitrogen
23   atom appearing at 2,802 cm^{-1} is disappeared in FT-IR spectrum of C-Dots. The peak at 3,272 cm^{-1} is N-
24   H stretching of secondary amine from piperazine. The peaks at 2,916, 2,915 and 2,834 cm^{-1} are
25   originating from C-H stretching of aliphatic group. The peak at 1,551 and 1,279 cm^{-1} is C=O stretching
26   from carboxylic acid originated from citric acid. The peaks between 1,020 and 1,220 cm^{-1} are allocated
27   to aliphatic amine. Actually, the peaks ranging from 455 to 1,551 cm^{-1} are exactly same as piperazine
28   citrate, and other peaks are originating from the dehydrated piperazine and 3-hydroxy-1,5-
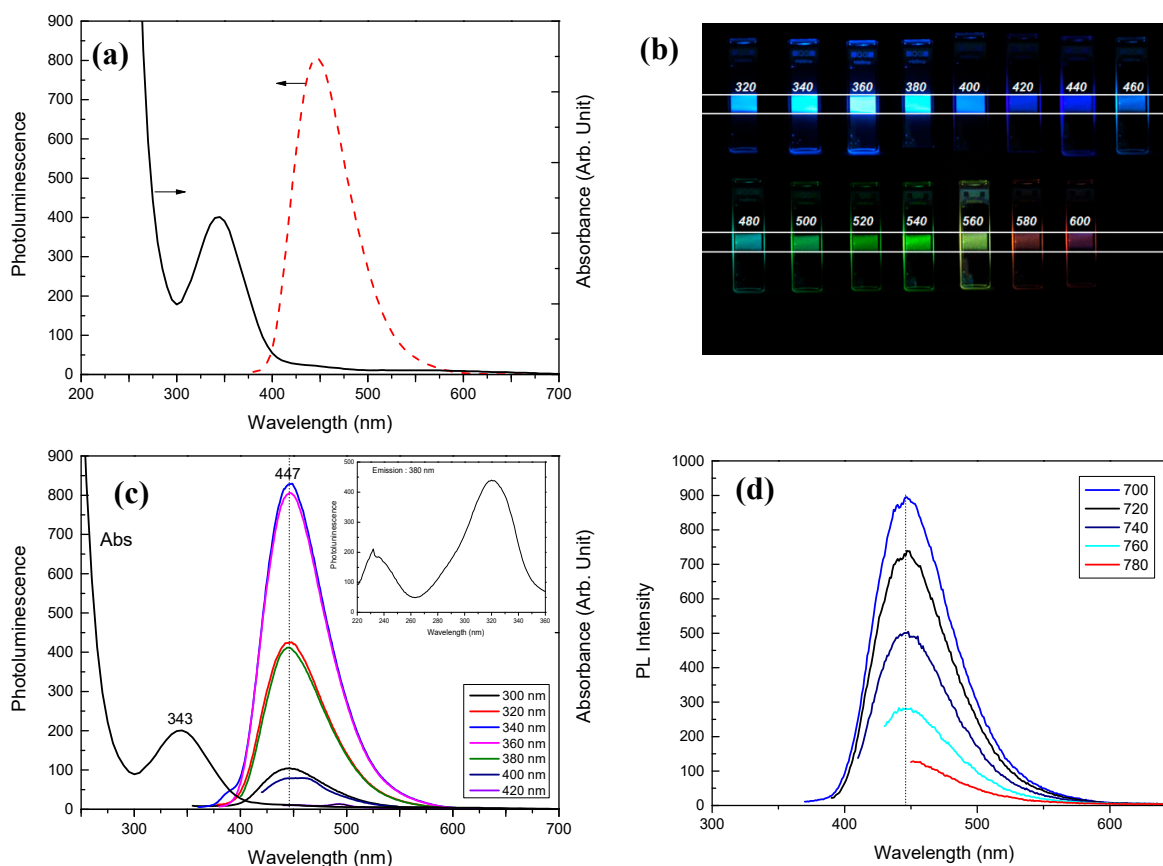29   di(piperazin-1-yl)-3-(piperazine-1-carbonyl)pentane-1,5-dione.
30

1   **Table 1.** Detailed experimental conditions and their PL QY.

Sample code	Citric acid (g)	Piperazine (g)	H$_2$O (mL)	Reaction Temp. (°C)	Reaction Time (hr)	QY (%)
13P160.5H-10	0.42	0.517	10	160	5	43.8
13P180.5H-10	0.42	0.517	10	180	5	63
13P200.5H-10	0.42	0.517	10	200	5	51.6
13P220.5H-10	0.42	0.517	10	220	5	58.9
13P160.5H-20	0.42	0.517	20	160	5	80
13∅P160.5H-20	0.21	0.2585	20	160	5	79.7
13∅P160.5H-10	0.21	0.2585	10	160	5	61
13P150.5H-20	0.42	0.517	20	150	5	79.8
13∅∅P150.5H-20	0.042	0.0517	20	150	5	57.5
13∅∅P150.5H-20-N	0.042	0.0517	20	150	5	61.6
13P150.5H-20-N	0.42	0.517	20	150	5	83.6

2   Description of sample code; ∅ means that the amount of precursors was reduced to 2 times. ∅∅
3   means that the amount of precursors was reduced to 10 times. N means that nitrogen gas was directly
4   flowing into the solution for 30 min before the reaction.
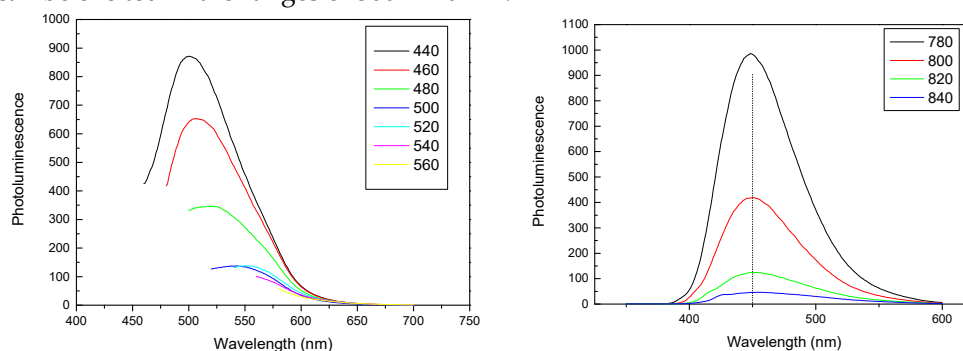

5   **Figure 2.** a) UV-vis absorption and PL emission spectra of C-Dots (13P150.5H-20-N). b) Optical images
6   of C-Dots solutions under the excitation with different wavelengths. c) UV/Vis absorption and PL
7   emission spectra and d) upconverted PL spectra of C-Dots prepared at 200 ˚C for 5 hrs with a molar
8   ration of citric acid: piperazine = 1:3. The PL emission spectra are recorded to identify the response on
9   longer excitation wavelengths from 300 to 420 nm and 700 to 780 nm.

10   *2.2. Photoluminescent properties of N-doped C-Dots*

11   Based on several experiments under different conditions (Table 1), oxygen and nitrogen had an
12   adverse effect on the formation of C-Dots. As the reaction temperature was increased, the PL QY

1 started to increase up to 63 % at 180 °C, and then decreased to 51 % at 200 °C, and increased back to
2 59 % at 220 °C. The amount of solvent (H$_2$O) is also very important factor for the synthesis of highly
3 luminescent C-Dots. When the concentration of the precursor decreases to half, the PL QY increases
4 from 44 % to 80 %. Continuous decrease in the concentration of the precursors, however, is expected
5 not to enhance the PL QY. As nitrogen gas was directly flowing into the solution for 30 min before
6 the reaction, PL QY showed an increase from 80 % to 84 %. Based on these results, it appears that the
7 oxygen and nitrogen content are relevant factors for the synthesis of C-Dots by hydrothermal reaction.
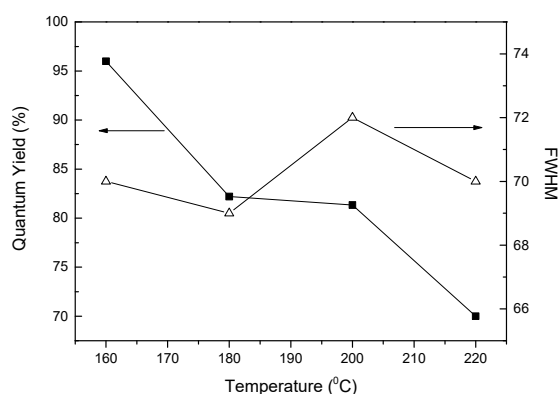8   The absorption and emission spectra of the synthesized C-Dots (Figure 2a) are comparable to
9 those previously reported ones. The absorption spectrum shows a peak centered at 343 nm. When
10 the C-Dots are excited at 360 nm, a strong PL emission peak located at 447 nm is observed. The full-
11 width at half-maximum (FWHM) excited at 360 nm is relatively narrow (~ 68 nm) indicating a
12 relatively small size distribution of the particles. Figure 2b shows the results at different excitation
13 illustrating the multicolor emission property of C-Dots. The emission color ranged from blue to red
14 making it a perfect candidate for fluorescent labeling in multiplexed biolabeling and bioimaging. To
15 explore the multicolor properties of as-synthesized C-Dots, a detailed PL was performed at different
16 excitation wavelengths. In most reported cases, PL emissions band maximum was red-shifted, i.e. the
17 PL emission shifted to the longer wavelengths with an increase in the excitation wavelength. The as-
18 prepared C-Dots, however, showed an excitation-independent PL feature.[15] Figure 2c shows the
19 PL spectra excited over a wide range. The spectra showed similar peak wavelengths with a strong
20 emission band centered at approximately 447 nm as it was excited from 300 - 420 nm. It means that
21 the particle size distribution of the given C-Dots was a highly monodispersed ones comparable to the
22 previous reported ones. The excitation dependent emission was mainly attributed to the different
23 particle size and a considerable distribution of emissive trap sites on each C-Dots.[16] Some of the
24 works reported that different sizes of C-Dots with different masses can be sorted using so-called size
25 classification process by gel electrophoresis (PAGE)[17] and they showed that the as prepared C-Dots
26 are composed of particles of different sizes in one batch. In this work, majority of the population of
27 C-Dots can be excited in the ranges of 300 - 420 nm.

28 **Figure 3.** a) PL emission spectra and b) upconverted PL spectra of C-Dots prepared at 200 °C for 5 hrs
29   with a molar ration of citric acid: piperazine = 1:3. The PL emission spectra are measured at high
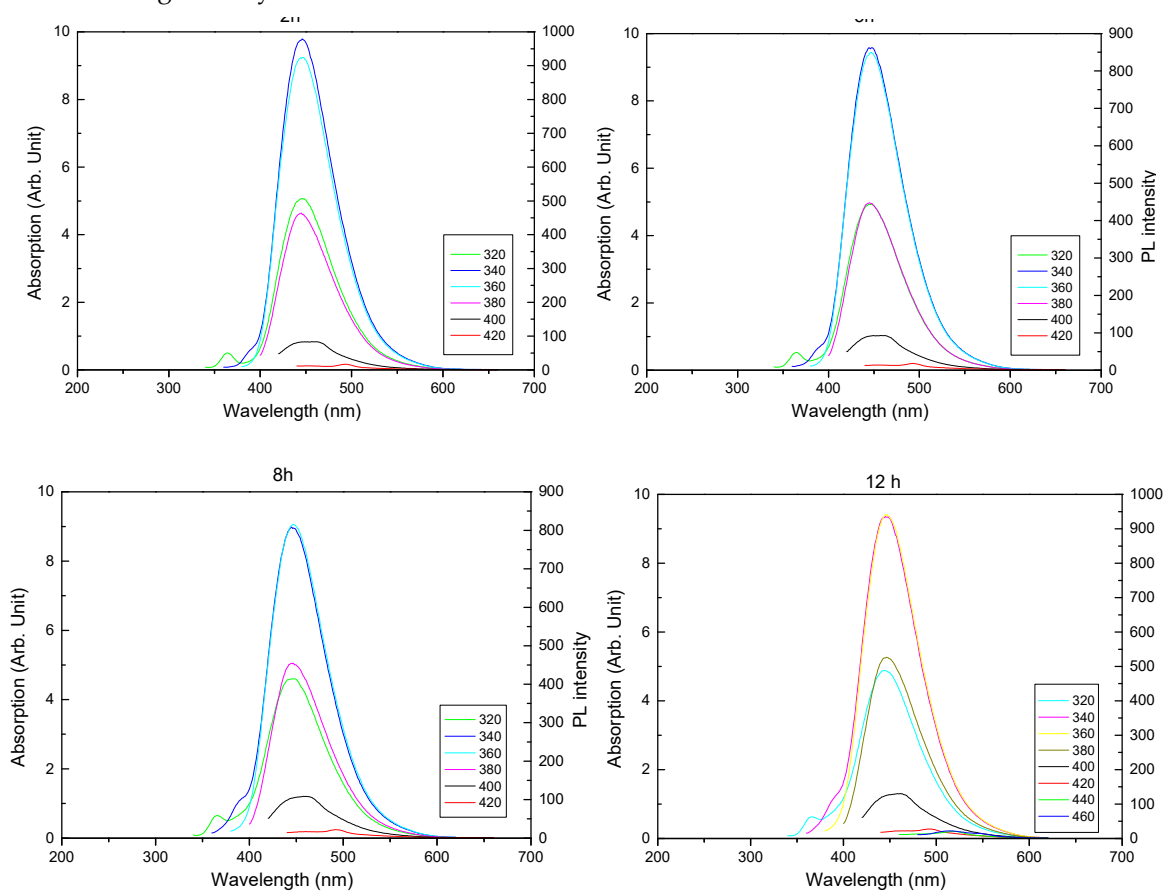30   concentration.

31   To identify the emission spectra at higher wavelengths, high concentration of the C-Dots (×100)
32 was used to measure the PL intensity within the excitation wavelength of 440 – 560 nm (Figure 3). It
33 shows a typical wavelength dependent PL properties over emission wavelengths ranging from blue
34 (450 nm) to red (570 nm). Besides exhibiting strong downconversion of PL properties, the obtained
35 C-Dots showed strong upconversion fluoresce simultaneously (Figure 2d and 3 a). The PL spectra
36 are almost unchanged at the excitation wavelengths from 700 nm to 780 nm, the upconversion
37 fluoresce are also located at λ_{em} = 447 nm, which is the same as downconversion peaks with a maximal
38 excitation wavelength at 700 nm. High concentration of the C-Dots was utilized to measure the PL
39 intensity on excitation wavelength ranging from 780 nm to 840 nm as shown in Figure 3 b; the
40 upconversion PL spectra showed an excitation-independent PL property which is different from the
41 downconversion PL spectra. Both the downconversion and upconversion results imply that the as-

1   prepared C-Dots can be employed to enhance the efficiency of absorption in various light spectra.
2

3

Figure 4. Quantum yield (QY) and Full Width at Half Maximum (FWHM) of C-Dots prepared at 160, 180, 200 and 220 ºC for 5 hrs with a molar ratio of citric acid: piperazine = 1:3. The peaks for QY are taken at the excitation wavelength of 360 nm.

7   The FWHM is relatively narrow (about 68 - 72 nm), which indicates a relatively small size
8   distribution of the C-Dots as shown in Figure 4.   When reaction time was increased from 2 to 12 hrs,
9   PL intensities were linearly decreased; whereas, excitation-independent PL property appeared at low
10   concentration by increasing the reaction time as shown in Figure 5. It is obvious that the particle sizes
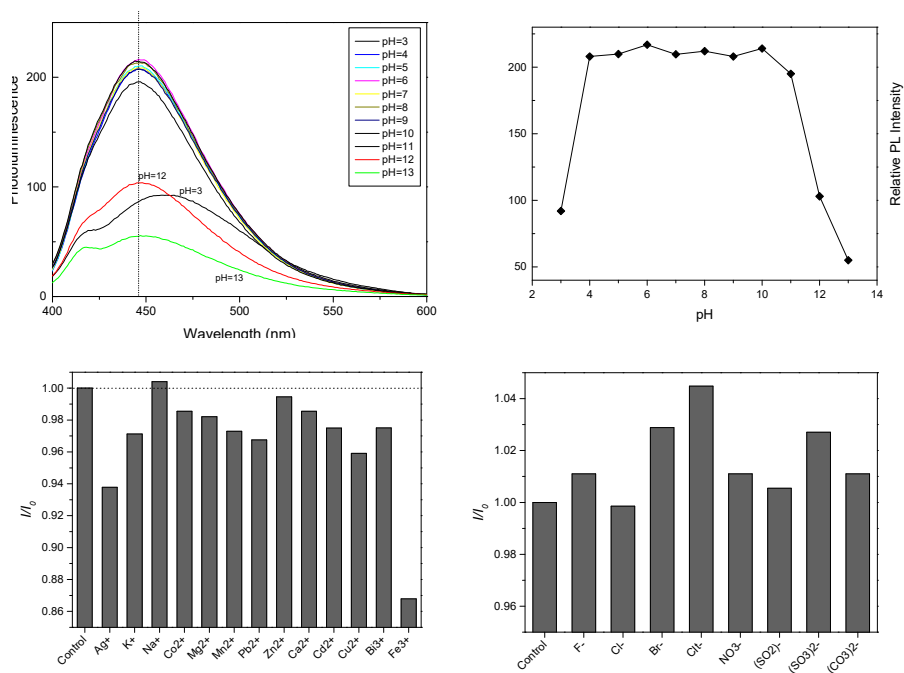11   of C-Dots are gradually increased as the reaction time is increased.

12

13

Figure 5. PL emission spectra of C-Dots prepared at 200 ℃ for 2 hrs, 5 hrs, 8 hrs, and 12 hrs with a molar ratio of citric acid: piperazine = 1:3. The PL emission spectra are recorded to identify the response on longer excitation wavelengths from 320 to 460 nm.

1　　　　Figures 6a and 6b show the variation of PL intensity of the C-Dots influenced by pH. pH of the
2　　solution was obviously affected in highly acidic and in alkali regions; whereas, the C-Dots were
3　　reasonably stable PL intensities in the pH range of 4 -11. These characteristic properties of C-Dots are
4　　totally prominent comparing to semiconductor based quantum dots (QDs) and can be applicable to
5　　the areas of biosensing and bioimaging. Figure 6c shows PL quenching effect of various metal ions
6　　with each being at a concentration of 50 µM (i.e. Ag^+, K^+, Na^+, Co^{2+}, Mg^{2+}, Mn^{2+}, Pb^{2+}, Pb^{2+}, Zn^{2+}, Ca^{2+},
7　　Cd^{2+}, Cu^{2+}, Bi^{3+} and Fe^{3+}), were added into C-Dots optical density of 0.05 measured by UV
8　　spectrophotometer. All the metal ions are quenching the PL intensity except Na^+. Primarily, K^+, Co^{2+},
9　　Mg^{2+}, Mn^{2+}, Pb^{2+}, Pb^{2+}, Zn^{2+}, Ca^{2+}, Cd^{2+}, Cu^{2+} and Bi^{3+} are interacted with carboxylic group from citric
10　　acid. Furthermore, other chemical reactions are involved for Ag^+ and Fe^{3+} such as metal complex and
11　　cheating. The PL of the C-Dots is seriously quenched by Fe^{3+} ions due to the formation of complexes
12　　between piperazine of the C-Dots and Fe^{3+} ions. It has been well reported that the quantitative
13　　analysis of piperazine derivatives by chelates with iron (III) and can be identified by
14　　spectrophotometric and potentiometric methods. [18] In addition, it has been well known that the
15　　compound of Cd^{2+} and Co^{2+} halides with piperazine include the linear Cd^{2+} and zigzag polymer
16　　chains formed because of the bridging nitrogen atoms if the piperazine ligand. Ag^+ ions with
17　　piperazine is also of polymeric structure.[19] We believe that the enhancement of PL of the C-Dots
18　　with Na^+ is derived from the photon induced electron transfer (PET) mechanism. In this model, ions
19　　with different d-electronic configuration exhibit PET or internal charge transfer between the
20　　combined ions and C-Dots.[20] Additionally, Ag can be reduced on the surface of C-Dots by exposing
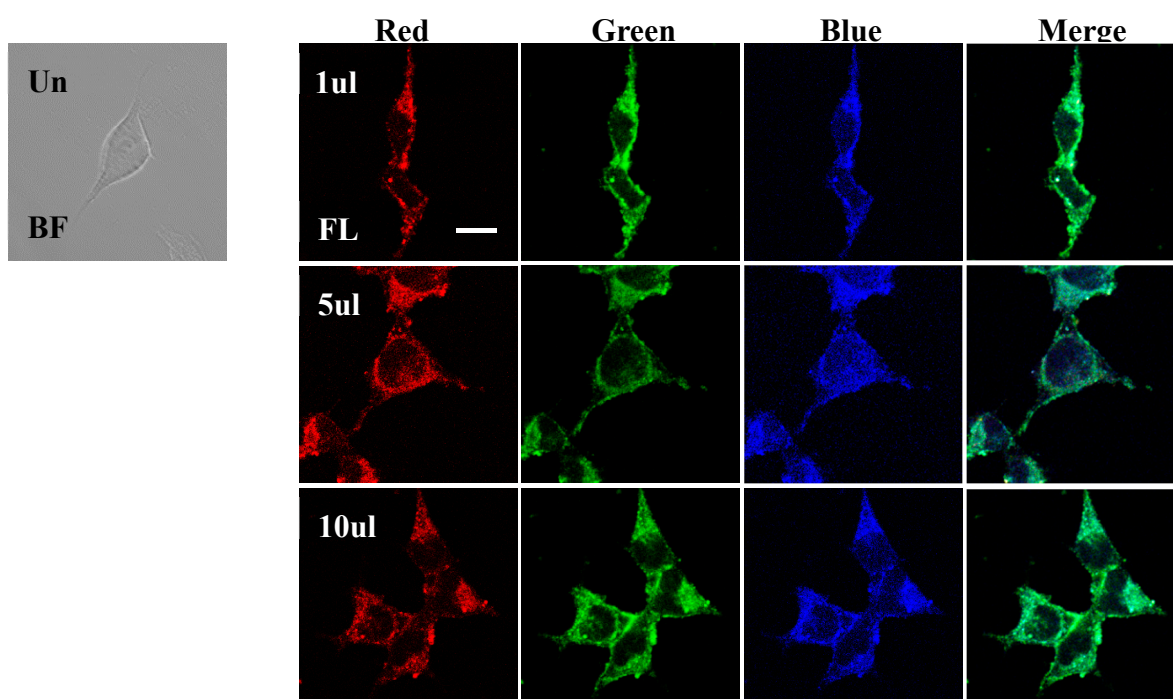21　　UV light, which enhances the surface plasmon resonance (SPR).

22　　**Figure 6.**　a) Effect of pH values on the PL spectra of C-Dots (13P150.5H-20-N) in aqueous solution.
23　　b) Variation of PL intensity depending on pH values. c) Comparison of PL intensities of C-Dots in the
24　　presence of metal ions (50uM M^+ and C-Dots (O.D=0.05) are incubated for 20 min). d) Comparison of
25　　PL intensities of C-Dots in the presence of sodium anions (50uM sodium anions and C-Dots
26　　(O.D=0.05) are incubated for 20 min)

27　　　　The photoexcited C-Dots play an important role as an electron-donating capability with the
28　　reduction of Ag salt to the corresponding Ag nanoparticles on the surface of C-Dots.[21] Figure 6d
29　　shows the enhancement of PL intensity in the presence of anions, i.e. F^-, Cl^-, Br^-, Cit^-, NO_3^-, SO_2^-, SO_3^{2-}
30　　and CO_3^{2-}, of sodium salts. Interestingly, all the anions of sodium salts enhance the PL intensity except
31　　Cl^-. Based on the results from the addition of cations and anions to the C-Dots, the cations will not so
32　　seriously affect the PL intensity; instead, the anions in metal salts seriously do. Thus, the influence

1 between anion and cations can't be directly compared to other published works. Cations, anions and
2 their mixtures are the factors to stimulate the PL of C-Dots. Interestingly, citrate ion enhances the PL
3 intensity more than any other anions. It is because of the influence of unreacted piperazine or
4 piperazine citrate or citrate ions present as surrounding molecules, which exist as wide ranges of
5 non-covalent interactions consisting of hydrogen bonding (types of OH¨O, N-H¨O and C-H¨O) and
6 ion pairing interactions connecting the various components into supramolecular structures. There
7 are also C-H¨O and C-H¨π intermolecular interactions taking part in the stabilization.[22] For this
8 reason, the proton stimulated electrons are easily transferred to neighboring molecules which could
9 enhance PET.

10 *2.3. Multicolor imaging and labelling of N-doped C-Dots*

11   For evaluating the possible application of the C-Dots as a fluorescent biological probe which
12 possess the wide dosing window and multicolor property, we examined the intracellular localization
13 of C-Dots in HEK 293T cells after the C-Dots treatment for 4 hrs. Due to the PL QY of C-Dots, HEK
14 293T cells only needed to be incubated with the C-Dots at extremely low concentration to obtain the
15 fluorescence images. Figure 7 shows confocal microscopy image taken within the HEK 293T cells
16 when incubated with the C-Dots. Here, the laser excitation at 358, 488, and 594 nm gave out blue,
17 green, and red color emission, respectively. Interestingly, even after 2 hrs of irradiation the
18 fluorescence of C-Dots was maintained without any photobleaching which implied that they were
19 particularly suitable for long-term cellular imaging (data is not shown). The C-Dots were localized in
20 perinuclear vacuole-like structures with granular pattern in cytoplasm sparing the nucleus. No signs
21 of any morphological deterioration like nuclear shrinkage were observed, even when the cytotoxic
22 materials underwent endocytosis. As a result, the C-Dots have a relatively good biocompatibility. In
23 addition, the photoluminescence of C-Dots under all of excitation wavelengths were completely
24 merged. Notably, there was no difference in the C-Dots fluorescent intensities with different
25 concentrations of 1, 5, and 10 μL, which means that the C-Dots can stably fluoresce even in
26 significantly small amount. We suggest the C-Dots are highly suitable candidates for biological probe
27 with multiple advantageous properties such as having multicolored labeling potency, wide dosing
28 window, good biocompatibility, and do not undergo photobleaching.

29

30 **Figure 7.** Confocal fluorescence images of HEK 293T cells treated with C-Dots (13P150.5H-20-N). C-
31 Dots loaded HEK 293T cells are incubated for 4 hrs and the labeled cells are imaged under

1 fluorescence microscope. The cells are imaged under bright field (BF) and fluorescence (FL) mode
2 with confocal laser-scanning microscope. Images acquired with green color (488 nm excitation), red
3 color (594 nm excitation), and blue color (358 nm excitation). Images are representative of three
4 independent experiments with similar results. Scale bar, 10um

5 **3. Materials and Methods**

6 *3.1. Materials*

7   Citric acid anhydrous ($HOC(COOH)(CH_2COOH)_2$, 99.9%), iron(III) chloride hexahydrate ($FeCl_3$
8   · $6H_2O$, 98%), silver chloride ($AgCl_2$, 99%) cadmium Chloride hydrate ($CdCl_2 \cdot xH_2O$ 99.995%),
9   sulphuric acid (H_2SO_4, 95-98%) and calcium chloride ($CaCl_2$, 97%) were supplied by Sigma-Aldrich
10 Chemical Co. (St. Louis, U.S.A.). Quinine sulphate dihydrate ($H_2SO_4 \cdot 2H_2O$, 99%) were supplied by
11 Acros. Lead(II) Acetate Trihydrate ($C_4H_6O_4Pb \cdot 3H_2O$, 99%), Manganese(II) chloride tetrahydrate
12 ($MnCl_2 \cdot 4H_2O$, 98%), Copper(II) Nitrate Trihydrate ($Cu(NO_3)_2 \cdot 3H_2O$, 99%) were supplied by Daejung.
13 Magnessium sulfate heptahydrate ($MgSO_4 \cdot 7H_2O$, 99.5%) and Potassium chloride (KCl, 99.5%) were
14 is supplied by Junsei Chemicals (Chuo-Ku, Tokyo). Sodium Chloride (NaCl, 99.5%), bismuth nitrate
15 pentahydrate ($Bi(NO_3)_3 \cdot 5H_2O$, 99%), cobalt(II) sulfate heptahydrate ($CoSO_4 \cdot 7H_2O$, 99%), piperazine
16 ($C_4H_{10}N_2$, 99.5%), and zinc nitrate hexahydrate ($Zn(NO_3)_2 \cdot 6H_2O$, 98%) were purchased from Samchun
17 chemicals (Kyunggido, South Korea). All the chemicals were used without further purification. Triple
18 distilled and deionized water is used throughout.

19 *3.2. Preparation of Carbon Dots*

20   C-Dots were prepared by directly reacting the piperazine and citric acid. The procedure for
21 synthesizing C-Dots was as follows. 2 mmol citric acid and 6 mmol piperazine were added to 10 mL
22 double distilled water (DDW) in 20 mL tubular vial. For sample code 13P150.5H-20-N, nitrogen gas
23 was directly flowing into the solution for 30 min before the reaction. The rubber cap was inserted to
24 vial and transferred to Teflon-lined autoclave (50 mL volume). The rubber cap was tightly contact
25 with cap of Teflon container and further with a stainless outer cap. The sample loaded autoclave was
26 heated at 160, 180, 200 and 200 °C for 5 hrs. The dependence of the piperazine was measured by
27 changing the molar ratio of 1 to 4 against citric acid. The reaction time was varied for 2, 5, 8 and 12
28 hrs. After heating the samples for predefined duration, the autoclave was allowed to cool at room
29 temperature. The 200 uL C-Dots, 700 uL EtOH and 700 uL acetone were transferred to 2 mL E-tube
30 and centrifuged at 14,000 rpm for 5 min. Unreacted precursors were precipitated on the bottom of
31 the E-tube with a color of brown. The supernatant was dried and redispersed in DDW for further
32 analysis.

33 *3.3. Fluorescence quantum yield measurements*

34   The relative fluorescence quantum yield (Φ) of the C-dots was measured according to the
35 procedure of a reported method and calculated using the equation of $\Phi_x = \Phi_{std} I_x A_{std} \eta^2_x / I_{std} A_x \eta^2_{std}$. The
36 optical densities were measured on Mecasys Optizen Pop UV–vis spectrophometer. In the equation,
37 I_x and I_{std} are the fluorescence intensities of the C-dots and the standard, and A_x and A_{std} are the optical
38 densities of the C-dots and the standard, respectively. Quinine sulfate in 0.1 M H_2SO_4 was chosen as
39 a standard with a quantum yield Φ_{std} = 0.58 at 360 nm. η_x and η_{std} are the refractive index of the C-Dots
40 and the standard, respectively. The absorbencies of all the samples in 1.0 cm cuvette were kept under
41 0.05 at the excitation wavelength to minimize re-absorption effects.

42 *3.4. Immunofluorescence and Confocal Microscopy*

43   The potential for bioimaging of C-Dots was tested using HEK 293T cells. Approximately 10^5
44 HEK 293T cells were deposited on each coverslip (diameter=18mm) to form a sparsely distributed
45 layer of cells to ensure good exposure to C-Dots. HEK 293T cells were cultured using the DMEM
46 growth medium with 10 % fetal bovine serum at 37 °C with 5 % CO_2. All the HEK 293T cells were

incubated until approximately 70 % confluence was achieved. The mixture of carbon dots in the DMEM medium was added to each well. After 4 hrs of incubation in 5 % CO_2 at 37 °C, the C-Dots loaded HEK 293T cells were washed twice with PBS to remove extracellular C-Dots and were then fixed with 4 % paraformaldehyde in PBS for 10 min. After mounting, fluorescence images were acquired using a confocal laser-scanning microscope (LSM 700; Zeiss).

3.5. Flow Cytometry

HEK 293T cells were cultured in DMEM supplemented with 10% heat-inactivated FBS and antibiotics (100U/ml penicillin G and 100 mg/ml streptomycin) at 37 ℃ in 5% CO_2 humidified atmosphere. In order to measure the cellular uptake of carbon dots quantitatively, HEK 293T cells were seeded into 12-well plates at an initial density of 1×10^5 cells/well. Subsequently, cells were treated with different concentrations for 4h. We removed the media and washed cells with PBS (pH 7.4) three times. Then the cells were trypsinized and re-suspended in PBS (pH 7.4). The fluorescence of carbon dots in cells was evaluated by FACSCanto II flow cytometer, as directed by the manufacturer (Becton Dickinson). The mean fluorescence intensity of carbon dots was calculated for each sample. Flow cytometry data were collected using 10,000 cells and were analyzed using the FlowJo software (Tree Star, Inc.).

The detectors used were side scatter (SSC), forward scatter (FSC), and four different fluorescent detetors, with FL1 (FITC fluorescence emission), FL2 (PE fluorescence emission), FL3 (APC fluorescence emission) and FL4 (Alexa 700 fluorescence emission) set on different voltage. A negative control (solvent control, SC) was used for instrument set-up for the fluorescence channels.

1) FITC fluorescence from the carbon dots then was detected using the FL1 channel, with a 488 nm (515-545 nm) blue laser. 2) PE fluorescene from the carbon dots was recorded in the FL2 channel with a 488 nm (564-606nm) blue laser. 3) APC fluorescene from the carbon dots was recorded in the FL3 channel with a 633 nm (650-670nm) laser. 4) Alexa 700 fluorescene from the carbon dots was recorded in the FL4 channel with a 660 nm (640-719nm) red laser.

Data analysis was carried out with flowjo software obtained from BD Biocsiences (Sydney, Australia). For data analysis, histograms were created by gating on the events falling within the defined region. Samples of carbon dot were analyzed on the histogram and the mean value recorded (MFI value).

4. Conclusions

In this work, we have developed the synthetic strategy of highly photoluminescent C-Dots prepared by hydrothermal reaction of citric acid and piperazine as an alternative carbon source and nitrogen passivating agent. The as synthesized C-Dots have extremely high PL QY ca. 84 % and exhibit excitation and pH-dependent emission behaviors over the entire visible range, and have long-term photo stability. The C-Dots demonstrate enhanced cellular permeability and low cytotoxicity. The confocal fluorescence imaging of the HEK 293T cells treated with the C-Dots showed broad tunablity of the C-Dots as well as the robust photostability; thus, it can be applicable as a non-toxic probing agent to *in vitro* multicolor imaging applications.

Author Contributions: Min-Cheol Kim and Do Kyung Kim designed the experiments and wrote the paper; Kwang Sik Yu and Jwa-Jin Kim performed the experiments and wrote the paper; Seung Yun Han analyses the data; and Nam Seob Lee and Yeong Gil Jeong discussed the results.

Conflicts of Interest: The authors declare no conflict of interest.

1 References

1. Liu, R.; Wu, D.; Liu, S.; Koynov, K.; Knoll, W.; Li, Q. An aqueous route to multicolor photoluminescent carbon dots using silica spheres as carriers. *Angewandte Chemie International Edition* **2009**, *48*, 4598-4601.

2. Welsher, K.; Liu, Z.; Daranciang, D.; Dai, H. Selective probing and imaging of cells with single walled carbon nanotubes as near-infrared fluorescent molecules. *Nano Letters* **2008**, *8*, 586-590.

3. Xu, Y.; Wu, M.; Liu, Y.; Feng, X.-Z.; Yin, X.-B.; He, X.-W.; Zhang, Y.-K. Nitrogen-doped carbon dots: A facile and general preparation method, photoluminescence investigation, and imaging applications. *Chemistry – A European Journal* **2013**, *19*, 2276-2283.

4. Malik, M.A.; O'Brien, P.; Revaprasadu, N. A simple route to the synthesis of core/shell nanoparticles of chalcogenides. *Chemistry of Materials* **2002**, *14*, 2004-2010.

5. Zhan, Q.; He, S.; Qian, J.; Cheng, H.; Cai, F. Optimization of optical excitation of upconversion nanoparticles for rapid microscopy and deeper tissue imaging with higher quantum yield. *Theranostics* **2013**, *3*, 306-316.

6. Sun, Y.P.; Zhou, B.; Lin, Y.; Wang, W.; Fernando, K.A.S.; Pathak, P.; Meziani, M.J.; Harruff, B.A.; Wang, X.; Wang, H., *et al.* Quantum-sized carbon dots for bright and colorful photoluminescence. *Journal of the American Chemical Society* **2006**, *128*, 7756-7757.

7. Qiao, Z.-A.; Wang, Y.; Gao, Y.; Li, H.; Dai, T.; Liu, Y.; Huo, Q. Commercially activated carbon as the source for producing multicolor photoluminescent carbon dots by chemical oxidation. *Chemical Communications* **2010**, *46*, 8812-8814.

8. Liu, C.; Zhang, P.; Tian, F.; Li, W.; Li, F.; Liu, W. One-step synthesis of surface passivated carbon nanodots by microwave assisted pyrolysis for enhanced multicolor photoluminescence and bioimaging. *Journal of Materials Chemistry* **2011**, *21*, 13163-13167.

9. Zhang, Y.-Y.; Wu, M.; Wang, Y.-Q.; He, X.-W.; Li, W.-Y.; Feng, X.-Z. A new hydrothermal refluxing route to strong fluorescent carbon dots and its application as fluorescent imaging agent. *Talanta* **2013**, *117*, 196-202.

10. Borse, V.; Thakur, M.; Sengupta, S.; Srivastava, R. N-doped multi-fluorescent carbon dots for 'turn off-on' silver-biothiol dual sensing and mammalian cell imaging application. *Sensors and Actuators B: Chemical* **2017**, *248*, 481-492.

11. Wang, J.; Li, Q.; Zhou, J.; Wang, Y.; Yu, L.; Peng, H.; Zhu, J. Synthesis, characterization and cells and tissues imaging of carbon quantum dots. *Optical Materials* **2017**, *72*, 15-19.

12. Wang, F.; Xie, Z.; Zhang, H.; Liu, C.-y.; Zhang, Y.-g. Highly luminescent organosilane-functionalized carbon dots. *Advanced Functional Materials* **2011**, *21*, 1027-1031.

13. Xie, Z.; Wang, F.; Liu, C.-y. Organic–inorganic hybrid functional carbon dot gel glasses. *Advanced Materials* **2012**, *24*, 1716-1721.

14. Zhu, S.; Meng, Q.; Wang, L.; Zhang, J.; Song, Y.; Jin, H.; Zhang, K.; Sun, H.; Wang, H.; Yang, B. Highly photoluminescent carbon dots for multicolor patterning, sensors, and bioimaging. *Angewandte Chemie International Edition* **2013**, *52*, 3953-3957.

15. Zhuo, S.; Shao, M.; Lee, S.-T. Upconversion and downconversion fluorescent graphene quantum dots: Ultrasonic preparation and photocatalysis. *ACS Nano* **2012**, *6*, 1059-1064.

16. Sun, Y.-P.; Zhou, B.; Lin, Y.; Wang, W.; Fernando, K.A.S.; Pathak, P.; Meziani, M.J.; Harruff, B.A.; Wang, X.; Wang, H., *et al.* Quantum-sized carbon dots for bright and colorful photoluminescence. *Journal of the American Chemical Society* **2006**, *128*, 7756-7757.

17. Liu, H.; Ye, T.; Mao, C. Fluorescent carbon nanoparticles derived from candle soot. *Angewandte Chemie International Edition* **2007**, *46*, 6473-6475.

18. Abou-Attia, F.M.; Issa, Y.M.; Abdel-Gawad, F.M.; Abdel-Hamid, S.M. Quantitative determination of some pharmaceutical piperazine derivatives through complexation with iron(iii) chloride. *Il Farmaco* **2003**, *58*, 573-579.

19. Kokunov, Y.V.; Gorbunova, Y.E.; Kovalev, V.V. Coordination polymers of silver with piperazine and uncoordinated anions: Syntheses and crystal structures of [ag(c4h10n2)]ch3so3 and [ag(c4h10n2)]po2f2. *Russ J Coord Chem* **2011**, *37*, 95-99.

20. Chandra, S.; Pathan, S.H.; Mitra, S.; Modha, B.H.; Goswami, A.; Pramanik, P. Tuning of photoluminescence on different surface functionalized carbon quantum dots. *RSC Advances* **2012**, *2*, 3602-3606.

21. Choi, H.; Ko, S.-J.; Choi, Y.; Joo, P.; Kim, T.; Lee, B.R.; Jung, J.-W.; Choi, H.J.; Cha, M.; Jeong, J.-R., *et al.* Versatile surface plasmon resonance of carbon-dot-supported silver nanoparticles in polymer optoelectronic devices. *Nat Photon* **2013**, *7*, 732-738.

22. Aghabozorg, H.; Mahfoozi, F.; Sharif, M.A.; Shokrollahi, A.; Derki, S.; Shamsipur, M.; Khavasi, H.R. A proton transfer self-associated compound from benzene-1,2,4,5-tetracarboxylic acid and piperazine and its cobalt(ii) complex: Syntheses, crystal structures and solution studies. *JICS* **2010**, *7*, 727-739.